

Mineral Acquisition Rates in Developing Enamel on Maxillary and Mandibular Incisors of Rats and Mice: Implications to Extracellular Acid Loading as Apatite Crystals Mature

Charles E Smith,^{1,2,3} Dennis Lee Chong,³ John D Bartlett,⁴ and Henry C Margolis⁵

ABSTRACT: The formation rates of mineral in developing enamel were determined by microweighing of incisors of mice and rats. Computations indicated that a large excess of hydrogen ions would result from creating apatite at the calculated rates. Enamel organ cells (ameloblasts), therefore, likely excrete bicarbonate ions to prevent pH in fluid bathing enamel from becoming too acidic.

Introduction: Protons (H^+) are generated whenever calcium and phosphate ions combine directly from aqueous solutions to form hydroxyapatite. Enamel is susceptible to potential acid loading during development because the amount of fluid bathing this tissue is small and its buffering capacity is low. The epithelial cells covering this tissue are also believed to form permeability barriers at times during the maturation stage when crystals grow at their fastest rates. The goal of this study was to measure the bulk weight of mineral present in rodent enamel at specific times in development and estimate the amount of acid potentially formed as the apatite crystals mature.

Materials and Methods: Upper and lower jaws of mice and rats were freeze-dried, and the enamel layers on the incisors were partitioned into a series of 0.5 mm (mouse) or 1.0 mm (rat) strips along the length of each tooth. The strips were weighed on a microbalance, ashed at 575°C for 18–24 h to remove organic material, and reweighed to determine the actual mineral weight for each strip.

Results and Conclusions: The data indicated that, despite differences in gross sizes and shapes of maxillary and mandibular incisors in rats and mice, the overall pattern and rates of mineral acquisition were remarkably similar. This included sharply increasing rates of mineral acquisition between the secretory and maturation stages, with peak levels approaching 40 $\mu\text{g}/\text{mm}$ tooth length. Computer modeling indicated that quantities of H^+ ions potentially generated as apatite crystals grew during the maturation stage greatly exceeded local buffering capacity of enamel fluid and matrix proteins. In other systems, bicarbonate ions are excreted to neutralize highly acidic materials generated extracellularly. Data from this study indicate that ameloblasts, and perhaps cells in other apatite-based hard tissues, use similar bicarbonate release mechanisms to control excess acid arising from mineral formation.

J Bone Miner Res 2004;20:240–249. Published online on October 11, 2004; doi: 10.1359/JBMR.041002

Key words: enamel, mineralization, pH control, carbonic anhydrase, bicarbonate ions

INTRODUCTION

THE MINERAL IN tooth enamel develops through a series of progressive steps that take days, weeks, or several months to complete, depending on species and crown size.⁽¹⁾ Among the earliest events to occur during enamel development is the formation and stabilization of thin apatite crystals within an organic-rich extracellular matrix composed predominately of amelogenins.^(2,3) This happens as ameloblasts move away from the dentinoenamel junction

and build up enamel thickness by appositional growth.⁽⁴⁾ Newly formed apatite crystals initially grow slowly in size until ameloblasts begin their cyclic modulations at the enamel surface during the maturation stage.⁽⁴⁾ This triggers a phase of accelerated protein degradation by matrix resident serine proteinases (currently called kallikrein 4 [KLK4]), which occurs as a prelude to more rapid volumetric growth of the apatite crystals, especially in terms of their thickness.^(4–7) The crystals eventually expand to occupy at least 80% of the volume of the enamel layer and comprise about 95% of mature enamel by weight.⁽⁸⁾ In rat incisors, it takes ameloblasts about 7.5 days to secrete the enamel layer and another 12–14 days for the enamel crystals to mature.⁽⁹⁾

The authors have no conflict of interest.

¹Laboratory for the Study of Calcified Tissues and Biomaterials, Département de Stomatologie, Faculté de Médecine Dentaire, Université de Montréal, Montreal, Canada; ²Department of Anatomy and Cell Biology, McGill University, Montreal, Canada; ³Faculty of Dentistry, McGill University, Montreal, Canada; ⁴Department of Cytokine Biology, The Forsyth Institute, Boston, Massachusetts, USA; ⁵Department of Biomineralization, The Forsyth Institute, Boston, Massachusetts, USA.

Protons are generated whenever apatite crystals grow in aqueous solutions at biological pH.⁽¹⁰⁾ This is because precursor forms of phosphate consumed in the chemical reaction at pH 7.0–7.4 are protonated either in the monobasic (H_2PO_4^-), or more commonly, the dibasic (HPO_4^{2-}) form.⁽¹¹⁾ In creating 1 mol of new apatite anywhere from 4 to 8, to as much as 14, moles of hydrogen ions can be released into the local environment. The exact amount formed depends on the phosphate precursor used and the stoichiometric amount of acid phosphate (v) and carbonate (w) incorporated into the forming apatitic mineral phase [generalized as $\text{Ca}_{10}(\text{PO}_4)_6(\text{OH})_2$ versus $\text{Ca}_{10-x}(\text{HPO}_4)_v(\text{CO}_3)_w(\text{PO}_4)_{6-x}(\text{OH})_{2-x}$ where $x = v + w$, when acid phosphate and carbonate contents are considered].^(10–12) Whereas quantities vary by species, there is always some acid phosphate and carbonated apatite present in enamel, especially at early times when the enamel first forms.^(8,13,14) Protons are also released when transient mineral species such as octacalcium phosphate convert into hydroxyapatite in aqueous solution at biological pH.^(15,16) The chemistry of these chemical reactions are so predictable that one well-accepted method for showing the formation of apatite from aqueous solutions involves simply monitoring the quantity of base (hydroxyl ions) required to keep solution pH at a constant level.^(10,17)

There is presently little information about how cells in various hard tissues deal with the acidification that occurs as a natural consequence of creating apatite crystals along a mineralization front. A common assumption is that the protons released by this process diffuse away or are rapidly neutralized by the high buffering capacity inherent to tissue fluids and blood. Whereas this could be true for bone, dentin, and cementum, developing enamel has a much higher potential for acid loading, because in addition to creating new apatite crystals as part of the appositional growth process, enamel is the only mammalian hard tissue where considerable postvolumetric expansion of crystals occurs after the appositional growth phase is completed.⁽⁴⁾ Also, based on findings from the only study reported to date, the amount of fluid bathing enamel is extremely small, its ionic composition is different from normal tissue fluid, and it possesses low buffering capacity.⁽¹⁸⁾ Although the epithelial cells covering developing enamel are known to be leaky to ions and various small molecules and proteins at certain times during amelogenesis, this epithelium otherwise maintains reasonably tight permeability barriers along the enamel surface, which restricts the free flow of ions into, or out of, enamel.⁽⁴⁾ This permeability barrier is associated with most of the secretory stage when the crystals are seeded and undergo their initial elongation and most of the maturation stage when the crystals actively grow in volume “underneath” ameloblasts that have highly invaginated apical ruffled borders.^(4,19,20)

The purpose of this study was to determine the weight of mineral acquired at sequential steps of amelogenesis in rodent incisors, and assuming that the mineral added is predominantly hydroxyapatite,^(8,12) to use these values to estimate the amount of acid potentially generated as enamel crystals form and mature. A second goal was to compare results on mineral acquisition for mandibular incisors to

those for maxillary incisors that have differences in timing of enamel development and in the ratios of the inner and outer portions of enamel rods eventually formed.^(9,21) A third goal was to compare results in rat to those for mice, which more commonly serve as an animal model for genetic manipulations of amelogenesis.^(22,23)

MATERIALS AND METHODS

Tissue preparation

All aspects in the handling, care, and usage of animals were done under guidelines specified by governmental agencies in the United States and Canada, and they were carried out under specific protocols approved by local animal care committees of McGill University and the Forsyth Institute. A group of 12 juvenile male Wistar rats (95 ± 5 g) and 6 adult C57BL6 mice of mixed sex were anesthetized with halothane and killed. Hemimandibles and hemimaxillae were removed, rapidly cleaned of adhering tissues, and immersed in liquid nitrogen for 5–7 h. The samples were freeze-dried at -55°C for 48 h (Labconco, Kansas City, MO, USA). The bone and enamel organs covering the incisors were removed, and the exposed enamel surfaces were wiped with Kimwipes (Kimberly-Clark Corp., Roswell, GA, USA). The enamel layer on each incisor was transected into a series of 0.5- (mice) or 1.0-mm-long (rats) strips from the apical aspect (least mature) to a point on the incisal (most mature) side of the tooth where the enamel was too hard to cut with a scalpel blade.⁽⁸⁾ The strips were removed, placed in separate 12-mm-diameter aluminum dishes (Thermo Electron Corp., Waltham, MA, USA), and further dried for about 12 h at 50°C .

Microweighing and ashing

Each enamel strip was weighed on a Mettler MT5 or UM2 microbalance (Mettler Toledo Canada, Mississauga, Ontario, Canada) and placed in a precleaned 15×15 -mm Coors crucible (1.3 ml capacity; Fisher Scientific, Nepean, Ontario, Canada). The crucibles were heated in a muffle furnace (Fisher Scientific) at 575°C for 18–24 h. The samples were cooled, and the residual material was reweighed (referred to as “ashed weight”). This procedure was done to remove organic material and bound water present in the enamel strips.⁽⁸⁾ Heating under these conditions is not known to cause any significant effect on hydroxyapatite,⁽²⁴⁾ although some CO_2 may be released from carbonated apatite⁽¹⁰⁾ and minor changes may occur to some crystal lattice parameters.⁽²⁵⁾ The “ashed weight” as determined by the above procedure therefore represents the amount of pure mineral present in a given enamel strip. Some ashed strips were dissolved in 0.5 M acetic acid, and the amounts of calcium and phosphorus were estimated spectrophotometrically as described by Hiller et al.⁽⁸⁾

Alignment of strips to the stages of enamel development

Enamel strips from mandibular incisors of rats and mice were aligned to the stages of amelogenesis using a molar reference line as described previously.⁽²⁶⁾ Enamel strips

from maxillary incisors were aligned by initially cutting away the apical portions of the tooth at a distance of 1.0 mm (mice) and 1.8 mm (rats) from the apical loop before the enamel organs were removed and making the strip dissections sequentially forward from this reference position once the enamel layer was exposed and cleaned.

Calculations from mineral weight data

Raw ashed weight values were used to compute changes in mineral weight per strip by progressive subtraction (e.g., weight change from strips 1→2 plotted at strip 2 location = ashed weight of strip 2 minus ashed weight of strip 1). These numbers were computed individually for each tooth and averaged together to derive means and variances. Titration curves were created from computer simulations using a previously described ion speciation software program.⁽²⁷⁾ The ionic composition of enamel fluid in rodent enamel is presently unknown and was therefore modeled using the only values currently available, which are for secretory stage pig enamel.⁽¹⁸⁾ This included 0.5 mM Ca^{2+} , 0.8 mM Mg^{2+} , 140 mM Na^+ , 20 mM K^+ , 146 mM Cl^- , 3.9 mM PO_4^{2-} , and 12 mM HCO_3^- at a starting pH of 7.26.⁽¹⁸⁾ The amount of fluid in enamel was estimated using values previously reported for rat.⁽⁴⁾ Fluid flow rates were arbitrarily expressed as mean fluid volume per millimeter (50 nl) per hour. The proton binding capacity of proteins in each enamel strip was computed from the following formula: (total weight of proteins in μg /molecular mass of amelogenin in nmoles) \times 15. This formula was based on a report by Ryu et al.⁽²⁸⁾ that 1 mol of recombinant amelogenin (rM179) binds 11–15 mol of protons. This approach slightly overestimated the potential contribution to proton binding made by the ~10% of matrix proteins that are nonamelogenins,^(3,4,11) because these proteins have a lower weight percent of histidine residues compared with amelogenins.^(11,29,30) The total weight of proteins in enamel strips was computed by subtracting the after-ashing weight from the starting dry weight of each strip. Because the molecular weights of amelogenins vary considerably in vivo (15,768–22,296 Da by MALDI mass spectrometry),⁽³¹⁾ an average mass value between the heaviest and lightest component of the main amelogenin group was used in this calculation (19,032 Da).^(31,32) This value is very close to the known mass of the main R180 isoform of amelogenin present in rat incisor enamel (20,373 Da by mass spectrometry).⁽³¹⁾ The amounts of acid released when creating stoichiometric hydroxyapatite with HPO_4^{2-} as precursor was computed from the following formula: (weight change per strip in micrograms/molecular mass of hydroxyapatite in nanomoles) \times 8, assuming that all 8 mol of hydrogen ions are released directly for each mole of hydroxyapatite formed and the molecular mass of stoichiometric hydroxyapatite is 1004.64 $[\text{Ca}_{10}(\text{PO}_4)_6(\text{OH})_2]$.^(10,11) Correction factors for amounts of acid phosphate and carbonated apatite present in developing enamel, which lowered estimates of hydrogen ions released from 8.00 to 5.52–7.06 mol/mol of mineral formed, were derived from speciation formulas reported by Aoba and Moreno⁽¹²⁾ for pig enamel (none are available for rat enamel). Correction factors for permeability changes related to the ameloblast modulation

cycle were derived from duration and percentage values for ruffle-/smooth-ended phases previously reported for rat.⁽³³⁾

RESULTS

Strip dissections

As expected, fewer enamel strips of equal length were obtained from maxillary incisors compared with mandibular incisors in rats (9 versus 12) and mice (7 versus 9), but the strip number ratio (max:man) was about equal at 1:1.3 in both species (Fig. 1). Fewer enamel strips were distributed over a much shorter tooth length in mouse incisors compared with rat incisors (Fig. 1). This was consistent with differences in absolute incisor lengths, which were about 1:2.3 comparing mice to rats (Fig. 1).⁽²¹⁾

Bulk changes in mineral content of enamel strips

The gross amount of mineral present in each enamel strip increased markedly from first to last strip of a series on all incisors (Fig. 2). No plateau in weight as described by others^(8,34) was reached before it was impossible to remove strips by freehand dissection (Figs. 1 and 2). Typically, about one-half of the total mineral weight change detected occurred almost exclusively within the last (most incisally positioned) three to four strips of a series on all incisors (Fig. 2). The weight of mineral present in the last (most mature) enamel strip of each series was slightly greater on mandibular incisors compared with maxillary incisors in rats and mice (differences were not significant; Fig. 2). The gross weight of mineral in the last enamel strip of each series were about 1.45 times greater in rat incisors compared with mouse incisors when raw values for mice were normalized on a per millimeter basis (Fig. 2). Ca:P molar ratios for rodent incisor enamel strips (data not shown) ranged from 1.5 to 1.7 and showed the same trends as those described by Hiller et al.⁽⁸⁾ for mandibular rat incisors.

Stepwise changes in mineral content of enamel strips

Plots of sequential changes in mineral weight across each series of strips indicated that the net mineral gain per strip was about four times greater at its peak level in the maturation stage compared with the secretory stage in all teeth examined (Fig. 3). Interestingly, the value at which mineral gain peaked within the maturation stage was similar on both maxillary and mandibular incisors in rats (~40 $\mu\text{g}/\text{mm}$ in rats; Fig. 3, top panels). This value was only slightly greater compared with peak levels estimated for mouse incisors when raw values were normalized on a per millimeter basis (~36 $\mu\text{g}/\text{mm}$ in mice; Fig. 3, bottom panels). There was a trend to reach a peak by the last (most mature) enamel strip in maxillary incisors of rats and mice (Fig. 3, left panels). In mandibular incisors of rats and mice, a peak was seen within one or two strips before the last (most mature) enamel strip in a series (Fig. 3, right panels).

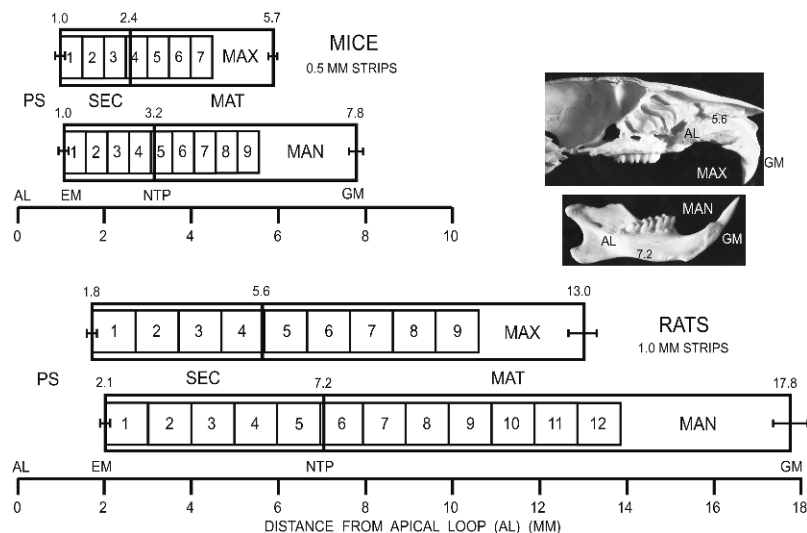


FIG. 1. Schematic representations of the embedded portions of maxillary (MAX) and mandibular (MAN) incisors from rats and mice showing the locations where enamel strips (numbered boxes) were soft enough to be removed from the tooth relative to the stages of amelogenesis (PS, presecretion, where cells differentiate; SEC, secretion, where the enamel layer is created to its full thickness; MAT, maturation, where apatite crystals grow markedly in size). The three numbers along the top of each long rectangle show the approximate starting and ending positions of the stages in millimeters relative to the apical loop (AL) (EM, point marking start for appositional growth of the enamel matrix; NTP, point marking the area where Tome's processes are no longer visible on ameloblasts; GM, gingival margin). (Inset) Mesial views of the left hemimaxilla and hemimandible of a rat showing the reference locations for AL and GM and transition from SEC to MAT (5.6 mm on MAX and 7.2 mm on MAN from the AL).

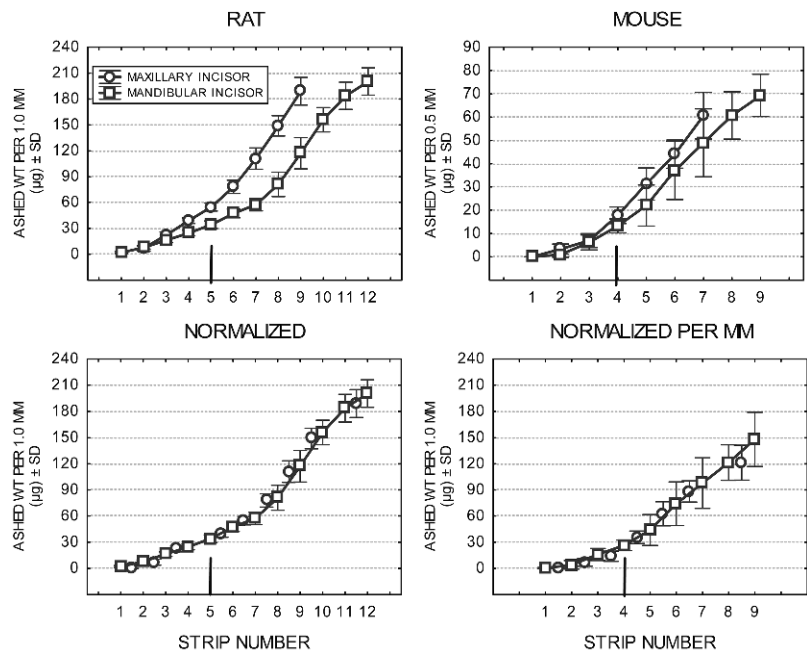


FIG. 2. Means plots ± SD of the average weight of mineral present in each enamel strip cut along the length of maxillary (○) and mandibular (□) incisors of rats (left panels) and mice (right panels) (see Fig. 1 for illustration of strip locations). Data in the top row are plotted by strip number, whereas data in the bottom row have been normalized by strip number to account for differences in tooth length between maxillary and mandibular incisors (strip number × 1.3). Data in the bottom right panel for mouse have also been normalized to express weight on a per millimeter basis (raw value × 2). The vertical line on the abscissa of each graph indicates the approximate boundary line between secretory and maturation stages on mandibular incisors.

Buffering capacity of enamel fluid and amounts of acid produced as apatite crystals grow

The left panel of Fig. 4 shows computer-generated estimates of the buffering capacity for increasing volumes of enamel fluid having ionic compositions as reported by Aoba and Moreno⁽¹⁸⁾ for porcine enamel. Plotted along the abscissa are estimates of the quantity of protons that would be released when forming 1 µg of new hydroxyapatite in aqueous solution. Estimates were derived using the two ionic forms of phosphate relevant at biological pH (H₂PO₄⁻ and HPO₄²⁻; see Simmer and Fincham⁽¹¹⁾). The right panel of Fig. 4 shows strip-by-strip estimates of the total amount

of acid that theoretically would be formed over about 37 h (1 mm = 37 h of renewal time in mandibular rat incisors⁽⁹⁾), creating hydroxyapatite from a HPO₄²⁻ precursor. Acid calculations were based on mineral weight gain. Data shown in the top right panel of Fig. 3. Figure 4 clearly suggest that the amount of protons released as a result of enamel mineral growth is greater than the local buffering capacity of enamel fluid or, when present, the buffering capacity of the matrix proteins. This is especially true during the mid-/late maturation stage when enamel fluid capacity is at its lowest and most of the proteins have been removed. However, this first approximation of acid production does not take into account certain key factors that

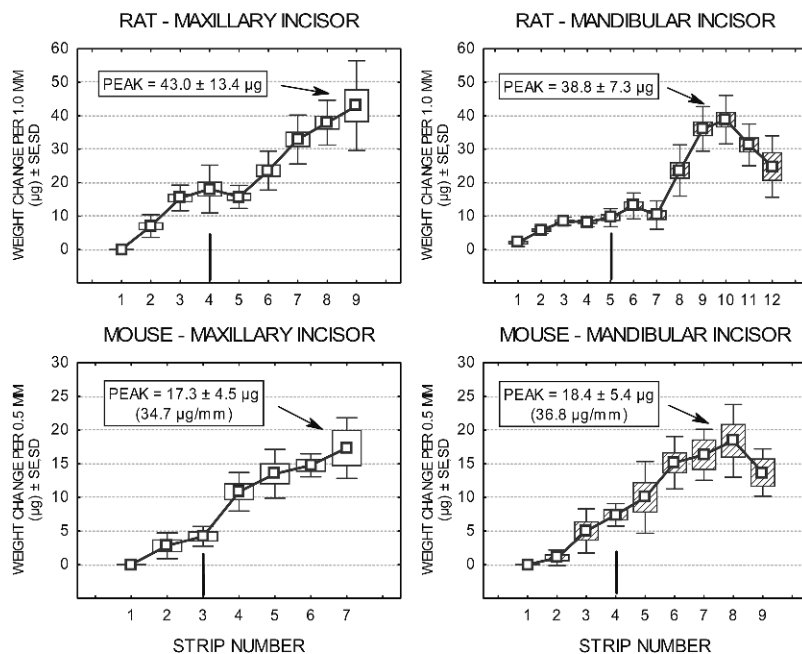


FIG. 3. Box plots (mean, square; SE, box around mean; SD, whiskers) of the weight changes in each enamel strip in the series in the maxillary (left panels) and mandibular (right panels) incisors of rats (top row) and mice (bottom row). The vertical line on the abscissa of each graph indicates the approximate boundary line between secretory and maturation stages.

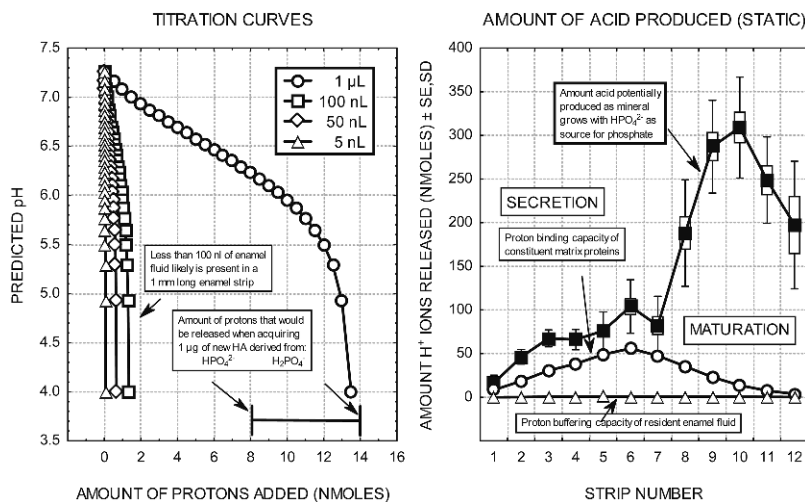


FIG. 4. Acid production vs. buffering potential. (Left panel) Computer simulations of changes in solution pH that would occur in various volumes of enamel fluid (5, 50, and 100 nL and 1 µL) after addition of amounts of hydrogen ions indicated along the abscissa (see Materials and Methods section). (Right panel) A box plot (mean [solid square] ± SE [box] and ± SD [whiskers]) of the total amount of hydrogen ions that could be generated over a 37-h period based on mineral weight gain data plotted in the top right panel of Fig. 3 for mandibular rat incisors assuming pure HA is formed using HPO_4^{2-} as phosphate source (1 mm = 37 h of renewal time for this incisor⁽⁹⁾). Plotted on the same graph are estimates of the buffering capacities associated with amounts of enamel fluid (triangles) and matrix proteins (circles) present within each strip.

directly influence the amount of protons actually formed or the amount of protons retained within the enamel layer. These issues are addressed in Fig. 5. This figure shows what happens when the first approximation of acid production (line 1) is corrected for amounts of acid phosphate and carbonate normally present in developing enamel (line 2) and then corrected for local protein and enamel fluid buffering including the assumption of replenishment of the enamel fluid at a rate of 50 nL/mm/h (line 3). The final correction (line 4) takes into account free diffusion of protons that could occur relative to leaky smooth-ended ameloblast during maturation stage modulation cycles (see Discussion section). Despite these corrections, excess acid is still predicted to exist across sequential 37-h intervals of the maturation stage that must be neutralized locally by enamel organ cells so that mineralization can proceed normally. Table 1 summarizes several aspects of mineral

growth, including consumption rates of calcium and phosphate ions needed to support apatite growth rates and predicted levels of acid produced during amelogenesis.

DISCUSSION

The value estimated in Table 1 for the weight of mineral present in a 1-mm-long strip of mature enamel on mandibular incisors of rats (230 µg/mm or 2.113 mg/mm³) compares favorably with mean mineral concentrations previously reported with other analytical approaches for these teeth by Hiller et al.⁽⁸⁾ (2.507 mg/mm³) and Wong et al.⁽³⁴⁾ (2.2–2.4 g/cm³). The “mature” enamel strip referred to in Table 1 is located about 2 mm away from the gingival margin (Fig. 1; strip 12 + 1 mm). It is expected this strip would gain some additional mineral in addition to this amount⁽³⁴⁾ until the yellow iron-based pigment typical of rodent incisors is

TABLE 1. MINERAL ACQUISITION, ION UPTAKE, AND POTENTIAL AMOUNT OF ACID RELEASED DURING AMELOGENESIS

	Rat (per mm)		Mouse (per 0.5 mm)	
	Max	Man	Max	Man
<i>Amount mineral acquired by stage (µg ± SD)</i>				
Secretion	38.8 ± 3.2	34.2 ± 4.4	7.0 ± 3.0	13.3 ± 3.0
Early maturation	39.4 ± 3.8	47.0 ± 7.1	24.3 ± 3.5	23.8 ± 6.3
Mid/late maturation	110.8 ± 11.7	119.2 ± 18.1	29.4 ± 6.1	32.2 ± 10.2
<i>Total</i>	189.0 ± 15.0	200.4 ± 15.8	60.7 ± 10.0	69.3 ± 9.1
Percent mineral by weight for <i>Total</i> *	87.5 ± 3.7%	88.3 ± 3.3%	88.4 ± 6.3%	87.9 ± 3.4%
Estimated mature weight† (per volume:)	226 µg	230 µg (2.113 mg/mm³)‡	76 µg	80 µg
<i>Rate parameters</i>				
Transition distance for change (mm)§				
Secretion	4	5	1.5	2
Early maturation	2	3	1	1
Mid/late maturation	3	4	1	1.5
<i>Total</i>	9	12	3.5	4.5
Transition time (days)¶				
Secretion	6.7	7.3	4.7	5.5
Early maturation	3.6	4.7	3.1	2.7
Mid/late maturation	5.4	6.2	3.1	4.1
<i>Total</i>	15.7	18.2	10.9	12.3
Acquisition rate of mineral (µg/day)				
Secretion	5.79	4.68	1.49	2.42
Early maturation	10.94	10.00	7.84	8.81
Mid/late maturation	20.52	19.23	9.48	7.85
<i>Total</i> (per volume:)	37.25	33.91 (312 µg/mm³/day)	18.81	19.08
Consumption rate of calcium (nmol/day)**				
Secretion	57.64	46.59	14.83	24.09
Early maturation	108.90	99.54	78.04	87.70
Mid/late maturation	204.26	191.42	94.37	78.14
<i>Total</i> (per volume:)	370.80	337.55 (3.102 µmol/mm³/day)	187.24	189.93
Consumption rate of phosphate (nmol/day)**††				
Secretion	34.58	27.95	8.90	14.45
Early maturation	65.34	59.72	46.82	52.62
Mid/late maturation	122.55	114.85	56.62	46.88
<i>Total</i> (per volume:)	222.47	202.52 (1.861 µmol/mm³/day)	112.34	113.95
Minimum acid output (H ⁺ ions released) (nmol/day)**				
Secretion	33.08	26.74	8.51	13.83
Early maturation	70.13	64.10	50.26	56.47
Mid/late maturation	144.20	135.14	66.62	55.17
<i>Total</i> (per volume:)	247.41	225.98 (2.076 µmol/mm³/day)	125.39	125.47

* Percent mineral by weight = (post-ashed weight/pre-ashed weight) × 100.

† The final mature weight for the enamel strips was estimated by computing the amount of mineral that would be added in advancing one additional strip position in an incisal direction (1 mm for rats and 0.5 mm for mice) and acquiring mineral at a rate indicated in the "Rate Parameters" column under "Acquisition rate of mineral—Mid/late maturation." The formula for this calculation = existing weight + ([distance/renewal rate] × mineral acquisition rate).

‡ Volumetric data are presently known only for mandibular incisors of rats; the volume of a 1-mm-long strip of almost mature enamel in these incisors = 0.10883 ± 0.0006 mm³ (see Fig. 4 in Smith⁽⁴⁾); the theoretical maximum weight of hydroxyapatite per cubic millimeter of enamel at 80% mineral by volume = density of HA (3.156 g/cm³) × 0.8 = 2.525 mg/mm³.

§ Shown in Fig. 1 as the number of strips (squares or rectangles) counted across each stage (×1 for rats or ×0.5 for mice).

¶ Based on incisor renewal rates given by Smith and Warshawsky⁽⁹⁾ for rats and Hwang and Tonna⁽⁵²⁾ for mice.

** Assuming the mineral that is ultimately formed exists predominately as hydroxyapatite (only about 2% of rat enamel is carbonated as estimated by Hiller et al.⁽⁸⁾); the weight of calcium in hydroxyapatite = HA weight × 0.398948.

†† The weight of phosphate in hydroxyapatite = HA weight × 0.567188.

** The amount of protons (H⁺ ions) that would be released with HPO₄²⁻ as phosphate source expressed in nmoles = ((HA weight/1.00464) × 8) × correction factor for amount of acid phosphate and carbonate present at stage of amelogenesis. Correction factors used were 0.7175 for secretion, 0.805 for early maturation, and 0.8825 for mid/late maturation based on data and speciation formulas determined in pig enamel by Aoba and Moreno⁽¹²⁾ (e.g., for mid/late maturation state enamel (M2), 9.26 Ca²⁺ + 5.48 HPO₄²⁺ + 0.50 HCO₃⁻ + 1.26 H₂O <-> Ca_{9.26}(HPO₄)_{0.22}(CO₃)_{0.50}(PO₄)_{5.26}(OH)_{1.26} + 7.06 H⁺; correction factor = 7.06/8.00 = 0.8825).

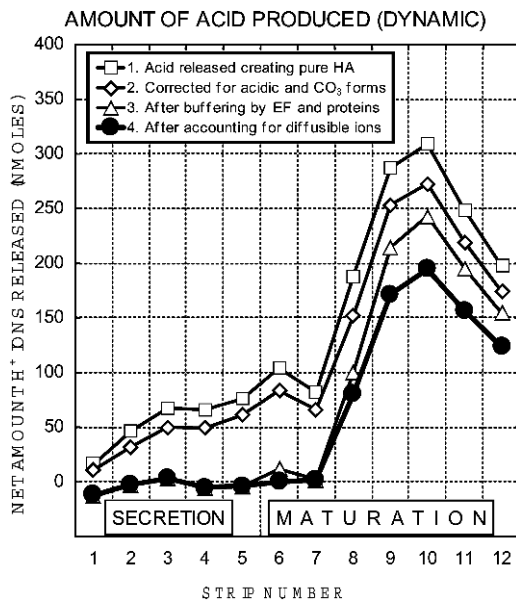


FIG. 5. Acid production vs. mineral phase formed and amounts of acid remaining after accounting for local buffering, enamel fluid exchange, and hydrogen ion diffusion. These means plots (symbols) show what happens when the static estimates of total acid production during amelogenesis shown in the right panel of Fig. 4 (line 1, □) are corrected for amounts of acid phosphate and carbonate present in forming enamel (line 2, ◇) and corrected for local buffering by matrix proteins and enamel fluid (EF), including the arbitrary assumption that enamel fluid may be refreshed at a rate of 50 nl/h (line 3, △). The fourth plot (●) takes into account the assumption that hydrogen ions are freely diffusible in areas covered by smooth-ended ameloblasts. This plot (●) is indicative of the amount of on-site bicarbonate buffering enamel organ cells (ameloblasts) would have to maintain over 37 h to counterbalance the acidity formed as enamel crystals mature.

added at its surface^(35,36) and this patch of enamel is carried forward by eruption into the oral cavity.⁽⁹⁾ Hence, although our mineral weight graphs did not reach plateaus (Fig. 2), we are confident that the weight values shown in Fig. 2, which form the basis of all acid release calculations presented in this study, are in good agreement with existing data for rodent incisors.

For the acid loading calculations (Figs. 4 and 5; Table 1), several assumptions had to be made and a number of variables had to be taken into account to make these estimates as reasonable as possible. These included selecting the form of phosphate most likely to be consumed in the chemical reactions leading to apatite (HPO_4^{2-} versus H_2PO_4^-), estimating buffering capacities of enamel fluid and matrix proteins, accounting for mineral incorporation of acid phosphate and for substitutions of carbonate for phosphate or hydroxide, as well as possible fluid flows and ion diffusion occurring in this system (Fig. 5). Results from this study would differ if the ionic composition of fluid in maturation stage enamel eventually proves to be different from secretory stage enamel or if the ionic composition of mouse and rat enamel fluid proves to be significantly different from that present in secretory stage pig enamel,⁽¹⁸⁾ on which all calculations were based. Even so, the data presented in Fig. 5 show unequivocally that the amount of acid potentially

released within the enamel layer as apatite crystals mature is substantial. It occurs in quantities large enough, in fact, to possibly terminate the mineralization process during enamel maturation unless additional local buffering capacity is provided by the epithelial cells covering this hard tissue.

Two general mechanisms exist by which enhanced extracellular buffering of free acid could be achieved in this system. One is by continuous circulation and replacement of the enamel fluid throughout the entire depth of the enamel layer to keep levels of bicarbonate ions at their maximum. This mechanism is most likely to occur in areas where the enamel organ cells maintain leaky junctional complexes such as during postsecretory transition or for brief periods during the maturation stage when ameloblasts lack the apical ruffled border and appear smooth-ended.⁽⁴⁾ Data in the left panel of Fig. 4 suggest that, for continuous fluid flow to compensate for acid stress arising during maturation, there would have to be at least 1 μl of fresh enamel fluid provided for each microgram of new apatite created or up to 30 μl of replacement enamel fluid per day in rat incisors based on the mineral acquisition rate data given in Table 1 for maturation stage enamel. This amount of enamel fluid is 60 times greater than the total volume of fluid estimated to be present throughout the entire enamel layer in vivo for rats,⁽⁴⁾ and it represents a very high fluid flow rate of ~ 20 nl/min. In addition, the volume of fluid filled spaces in the enamel layer decrease as the apatite crystals expand and mature.⁽⁴⁾ Therefore, the rate of replenishment of the enamel fluid would have to increase substantially over the course of enamel maturation to maintain optimum buffering efficiency. These large quantities of enamel fluid and fast flow rates seem to exclude fluid circulation as a practical and efficient method for neutralizing the excess acid.

A second, and in our opinion more likely, mechanism to supplement local buffering capacity is by continuous/periodic release of bicarbonate ions from ameloblasts directly into the enamel layer in amounts required to neutralize the excess hydrogen ions (H^+ [product of mineral formation] + HCO_3^- [excreted from cells] \leftrightarrow H_2O + CO_2).⁽⁴⁾ Such a mechanism implies that these cells not only must be able to "sense" local pH⁽³⁷⁾ and respond accordingly to the acid stress, but they also must have at the minimum one or more solute carrier proteins associated with bicarbonate transport^(38,39) embedded in their plasma membranes. They would also need one or more members of the carbonic anhydrase family of proteins to generate bicarbonate ions from CO_2 and water (reverse of reaction given above).⁽⁴⁰⁾

Biological precedents exist for "on demand" excretion of bicarbonate ions. The most notable example is in the gastrointestinal tract, where duct cells of the pancreas release enormous quantities of bicarbonate ions as a method to neutralize the highly acidic material exiting from the stomach.⁽⁴¹⁾ The duct cells use the high efficiency CA2 form of cytoplasmic carbonic anhydrase⁽⁴⁰⁾ to generate free bicarbonate ions that pass through the apical membranes through bicarbonate/chloride exchangers.⁽⁴¹⁾ The counter hydrogen ions formed from the reaction of CO_2 and water are moved out of the basolateral sides through sodium/

hydrogen exchangers where they are eventually neutralized by bicarbonate ions present in the surrounding tissue fluids and blood.⁽⁴¹⁾ The duct cells also express two membrane-embedded carbonic anhydrases, CA4 and CA12,⁽⁴⁰⁾ whose active sites project into the duct lumen from the apical membranes.⁽⁴¹⁾ The duct cells also secrete CA6,⁽⁴⁰⁾ which becomes part of the contents of the lumen and functions either to generate additional bicarbonate ions or to drive the neutralization reaction depending on conditions (H^+ [from stomach] + HCO_3^- [excreted by the duct cell] \leftrightarrow H_2O + CO_2).⁽⁴¹⁾ Similar bicarbonate-based mechanisms for neutralizing acid released from growing apatite crystals in enamel could easily exist for ameloblasts, and perhaps, other cells, creating apatite-based hard tissues. Existing literature suggests that maturation stage ameloblasts are especially rich in carbonic anhydrase activity and one of the isoforms present is CA2.^(42–44) Models for how the ameloblasts might excrete bicarbonate ions from their apical surfaces and “dispose” of excess cytoplasmic protons from their basolateral surfaces have been described.^(4,45)

Another factor that could influence the extent of the need to neutralize protons generated in the enamel layer during development revolves around the basic issue of the tightness/leakiness of permeability barriers maintained across the enamel surface by ameloblasts.^(4,19,20) This topic has been very controversial in part because of lack of systematic investigations and in part because the results of studies with large- and medium-size tracer molecules like albumin, horseradish peroxidase, and microperoxidase and small fluorescing tracer molecules like calcein, tetracycline, and xylenol orange or radiolabeled calcium and phosphate have not always agreed with the results of other studies carried out with lanthanum nitrate, especially regarding the tightness of cell junctions during the secretory stage of amelogenesis.⁽⁴⁾ However, in the case of the maturation stage, where the greatest potential for acid loading seems to exist (Fig. 5), many investigative approaches have consistently shown that ameloblasts maintain tight and impermeable apical junctions when they are ruffle-ended, and they have open and very leaky apical junctions but tight basal junctions when they are smooth-ended.⁽⁴⁾ Lanthanum impermeable junctions also seem to exist along the boundaries lines, where the narrow bands of smooth-ended ameloblasts abut the much larger patches of ruffle-ended ameloblasts.⁽⁴⁶⁾ It is on this basis that we concluded that free diffusion of hydrogen ions can occur outward over areas of enamel covered by smooth-ended ameloblasts but not those areas covered by ruffle-ended ameloblasts or where smooth-ended ameloblasts abut ruffle-ended ameloblasts.^(4,19,46,47) This is supported especially by findings from fluorescent tracer studies, where the smooth-ended ameloblast modulation bands are always very precisely and sharply delineated along the edges where they interface with the ruffle-ended ameloblasts after intravascular injections.⁽³³⁾ In addition, pH indicator dyes and direct micro-pH probings have consistently and repeatedly shown abrupt changes from mildly acidic to neutral pH at the boundaries between areas covered by ruffled-end and smooth-ended ameloblasts, respectively.^(1,45,48,49) These results are all consistent with the premise that lateral diffusion

of hydrogen ions from areas covered by ruffle-ended ameloblasts likely does not occur to any great extent into areas covered by smooth-ended ameloblasts. Hence, when a “diffusion window” opens during the smooth-ended phase of the modulation cycle,⁽³³⁾ it likely affects only those hydrogen ions contained directly “underneath” the smooth-ended cells. At any given moment in time, smooth-ended ameloblasts cover only 20% of the enamel surface,⁽³³⁾ and it is for these reasons that we estimated that only 20% of the acid load occurring during the maturation stage could be dispensed with by free diffusion (Fig. 5).

In summary, results from this study indicate that ameloblasts and associated papillary layer cells face a problem not only of having to transport enough calcium and phosphate ions to support mineral growth during enamel development, but also of having to deal with acidification that occurs as the apatite crystals mature. During the peak period of mineral growth in the maturation stage, amounts of acid are produced that are many orders of magnitude above the inherent buffering capacity of proteins and fluids present within the enamel layer. This suggests enamel organ cells must use various cytoplasmic and membrane-associate isoforms of carbonic anhydrase to generate bicarbonate ions that can be exported into the enamel layer to neutralize the excess acid being formed. Taking into account the fact that some ameloblasts die at the beginning as well as throughout the course of the maturation stage,⁽⁵⁰⁾ progressively fewer cells have to deal with progressively greater levels of pH and ion transport stress (four to five times more) as maturation proceeds. Because the enamel organ exists as a stratified epithelium, the ameloblasts must also act in a very coordinated fashion with their neighboring papillary layer cells to carry out these tasks efficiently.⁽⁵¹⁾ The results from this study further suggest that there may be times during development when any cell making an apatite-based hard tissue may have to excrete bicarbonate ions to counterbalance excess protons generated as part of the mineralization process.

ACKNOWLEDGMENTS

This study was supported by NIDCR Program Project Grant DE-13237.

REFERENCES

1. Nanci A 2003 Ten Cate's Oral Histology: Development, Structure, and Function, 6th ed., Mosby, St Louis, MO, USA.
2. Fincham AG, Moradian-Oldak J, Simmer JP 1999 The structural biology of the developing dental enamel matrix. *J Struct Biol* **126**:270–299.
3. Moradian-Oldak J 2001 Amelogenins: Assembly, processing and control of crystal morphology. *Matrix Biol* **20**:293–305.
4. Smith CE 1998 Cellular and chemical events during enamel maturation. *Crit Rev Oral Biol Med* **9**:128–161.
5. Robinson C, Brookes SJ, Kirkham J, Bonass WA, Shore RC 1996 Crystal growth in dental enamel: The role of amelogenins and albumin. *Adv Dent Res* **10**:173–180.
6. Bartlett JD, Simmer JP 1999 Proteinases in developing dental enamel. *Crit Rev Oral Biol Med* **10**:425–441.
7. Hu JCC, Sun XL, Zhang CH, Liu SX, Bartlett JD, Simmer JP 2002 Enamelysin and kallikrein-4 mRNA expression in developing mouse molars. *Eur J Oral Sci* **110**:307–315.

8. Hiller CR, Robinson C, Weatherell JA 1975 Variations in the composition of developing rat incisor enamel. *Calcif Tissue Res* **18**:1–12.
9. Smith CE, Warshawsky H 1975 Cellular renewal in the enamel organ and the odontoblast layer of the rat incisor as followed by radioautography using ³H-thymidine. *Anat Rec* **183**:523–562.
10. Elliott JC 1994 Structure and Chemistry of the Apatites and Other Calcium Orthophosphates. Elsevier, Amsterdam, The Netherlands.
11. Simmer JP, Fincham AG 1995 Molecular mechanisms of dental enamel formation. *Crit Rev Oral Biol Med* **6**:84–108.
12. Aoba T, Moreno EC 1992 Changes in the solubility of enamel mineral at various stages of porcine amelogenesis. *Calcif Tissue Int* **50**:266–272.
13. Shimoda S, Aoba T, Moreno EC 1991 Changes in acid-phosphate content in enamel mineral during porcine amelogenesis. *J Dent Res* **70**:1516–1523.
14. Siew C, Gruninger SE, Chow LC, Brown WE 1992 Procedure for the study of acidic calcium phosphate precursor phases in enamel mineral formation. *Calcif Tissue Int* **50**:144–148.
15. Iijima M 2001 Formation of octacalcium phosphate in vitro. In: Eanes ED, Chow LC (eds.) *Octacalcium Phosphate*. Karger, Basel, Switzerland, pp. 17–49.
16. Eidelman N, Eanes ED 2001 Role of OCP in biological processes. In: Eanes ED, Chow LC (eds.) *Octacalcium Phosphate*. Karger, Basel, Switzerland, pp. 50–75.
17. Hunter GK, Kyle CL, Goldberg HA 1994 Modulation of crystal formation by bone phosphoproteins: Structural specificity of the osteopontin-mediated inhibition of hydroxyapatite formation. *Biochem J* **300**:723–728.
18. Aoba T, Moreno EC 1987 The enamel fluid in the early secretory stage of porcine amelogenesis: Chemical composition and saturation with respect to enamel mineral. *Calcif Tissue Int* **41**:86–94.
19. Takano Y 1995 Enamel mineralization and the role of ameloblasts in calcium transport. *Connect Tissue Res* **33**:127–137.
20. Hubbard MJ 2000 Calcium transport across the dental enamel epithelium. *Crit Rev Oral Biol Med* **11**:437–466.
21. Moinichen CB, Lyngstadaas SP, Risnes S 1996 Morphological characteristics of mouse incisor enamel. *J Anat* **189**:325–333.
22. Gibson CW, Yuan ZA, Hall B, Longenecker G, Chen EH, Thyagarajan T, Sreenath T, Wright JT, Decker S, Piddington R, Harrison G, Kulkarni AB 2001 Amelogenin-deficient mice display an amelogenesis imperfecta phenotype. *J Biol Chem* **276**:31871–31875.
23. Caterina JJ, Skobe Z, Shi J, Ding YL, Simmer JP, Birkedal-Hansen H, Bartlett JD 2002 Enamelysin (matrix metalloproteinase 20)-deficient mice display an amelogenesis imperfecta phenotype. *J Biol Chem* **277**:49598–49604.
24. Takagi T, Sasaki S, Aoki H, Kikuchi M 1993 Crystal chemistry of secretory stage in developing enamel. *Jpn J Oral Biol* **35**:338–348.
25. Hiller JC, Thompson TJU, Evison MP, Chamberlain AT, Wess TJ 2003 Bone mineral change during experimental heating: An X-ray scattering investigation. *Biomaterials* **24**:5091–5097.
26. Smith CE, Nanci A 1989 A method for sampling the stages of amelogenesis on mandibular rat incisors using the molars as a reference for dissection. *Anat Rec* **225**:257–266.
27. Moreno EC, Margolis HC 1988 Composition of human plaque fluid. *J Dent Res* **67**:1181–1189.
28. Ryu OH, Hu CC, Simmer JP 1998 Biochemical characterization of recombinant mouse amelogenins: Protein quantitation, proton absorption, and relative affinity for enamel crystals. *Connect Tissue Res* **39**:207–214.
29. Krebsbach PH, Lee SK, Matsuki Y, Kozak CA, Yamada KM, Yamada Y 1996 Full-length sequence, localization, and chromosomal mapping of ameloblastin - A novel tooth-specific gene. *J Biol Chem* **271**:4431–4435.
30. Hu CC, Simmer JP, Bartlett JD, Qian Q, Zhang C, Ryu OH, Xue J, Fukae M, Uchida T, MacDougall M 1998 Murine amelogenin: CDNA and derived protein sequences. *Connect Tissue Res* **39**:351–365.
31. Chen WY, Bell AW, Simmer JP, Smith CE 2000 Mass spectrometry of native rat amelogenins: Primary transcripts, secretory isoforms, and C-terminal degradation. *J Dent Res* **79**:840–849.
32. Fincham AG, Moradian-Oldak J 1996 Comparative mass spectrometric analyses of enamel matrix proteins from five species suggest a common pathway of post-secretory proteolytic processing. *Connect Tissue Res* **34**:5:205–210.
33. Smith CE, McKee MD, Nanci A 1987 Cyclic induction and rapid movement of sequential waves of new smooth-ended ameloblast modulation bands in rat incisors as visualized by polychrome fluorescent labeling and GBHA-staining of maturing enamel. *Adv Dent Res* **1**:162–175.
34. Wong FSL, Elliott JC, Davis GR, Anderson P 2000 X-ray microtomographic study of mineral distribution in enamel of mandibular rat incisors. *J Anat* **196**:405–413.
35. Halse A, Selvig KA 1974 Mineral content of developing rat incisor enamel. *Scand J Dent Res* **82**:40–46.
36. Karim AC, Warshawsky H 1984 A radioautographic study of the incorporation of iron 55 by the ameloblasts in the zone of maturation of rat incisors. *Am J Anat* **169**:327–335.
37. Lahiri S, Forster RE II 2003 CO₂/H⁺ sensing: Peripheral and central chemoreception. *Int J Biochem Cell Biol* **35**:1413–1435.
38. Sterling D, Casey JR 2002 Bicarbonate transport proteins. *Biochem Cell Biol* **80**:483–497.
39. Hediger MA, Romero MF, Peng JB, Rolfs A, Takanaga H, Bruford EA 2004 The ABCs of solute carriers: Physiological, pathological and therapeutic implications of human membrane transport proteins. *Pflugers Arch* **447**:465–468.
40. Chegwiddden WR, Carter ND 2000 Introduction to the carbonic anhydrases. In: Chegwiddden WR, Carter ND, Edwards YH (eds.) *The Carbonic Anhydrases*. Birkhäuser Verlag, Basel, Switzerland, pp. 13–28.
41. Nishimori I, Fujikawa-Adachi K, Onishi S, Hollingsworth MA 1999 Carbonic anhydrase in human pancreas: Hypotheses for the pathophysiological roles of CA isozymes. *Ann NY Acad Sci* **880**:5–16.
42. Sugimoto T, Ogawa Y, Kuwahara H, Shimazaki M, Yagi T, Sakai A 1988 Histochemical demonstration of carbonic anhydrase activity in the odontogenic cells of the rat incisor. *J Dent Res* **67**:1271–1274.
43. Lin HM, Nakamura H, Noda T, Ozawa H 1994 Localization of H⁺-ATPase and carbonic anhydrase II in ameloblasts at maturation. *Calcif Tissue Int* **55**:38–45.
44. Toyosawa S, Ogawa Y, Inagaki T, Ijuhin N 1996 Immunohistochemical localization of carbonic anhydrase isozyme II in rat incisor epithelial cells at various stages of amelogenesis. *Cell Tissue Res* **285**:217–225.
45. Sui W, Boyd C, Wright JT 2003 Altered pH regulation during enamel development in the cystic fibrosis mouse incisor. *J Dent Res* **82**:388–392.
46. Josephsen K 1984 Lanthanum tracer study on permeability of ameloblast junctional complexes in maturation zone of rat incisor enamel organ. In: Fearnhead RW, Suga S (eds.) *Tooth Enamel IV*. Elsevier Science Publishers, Amsterdam, The Netherlands, pp. 251–255.
47. Kawamoto T, Shimizu M 1997 Pathway and speed of calcium movement from blood to mineralizing enamel. *J Histochem Cytochem* **45**:213–230.
48. Smith CE, Issid M, Margolis HC, Moreno EC 1996 Developmental changes in the pH of enamel fluid and its effects on matrix-resident proteinases. *Adv Dent Res* **10**:159–169.
49. Sasaki S, Takagi T, Suzuki M 1991 Cyclical changes in pH in bovine developing enamel as sequential bands. *Arch Oral Biol* **36**:227–231.

50. Smith CE, Warshawsky H 1977 Quantitative analysis of cell turnover in the enamel organ of the rat incisor, evidence for ameloblast death immediately after enamel matrix secretion. *Anat Rec* **187**:63–98.
51. Ohshima H, Maeda T, Takano Y 1998 Cytochrome oxidase activity in the enamel organ during amelogenesis in rat incisors. *Anat Rec* **252**:519–531.
52. Hwang WSS, Tonna EA 1965 Autoradiographic analysis of labeling indices and migration rates of cellular component of mouse incisors using tritiated thymidine (H3TDR). *J Dent Res* **44**:42–53.

Address reprint requests to:
Charles E Smith, DDS, PhD
Faculté de Médecine Dentaire
Université de Montréal
C.P. 6128, Succ. Centre-ville
Montreal, Quebec, Canada H3C 3J7
E-mail: ce.smith@umontreal.ca

Received in original form October 24, 2003; revised form August 1, 2004; accepted September 14, 2004.